

## On magma chamber evolution during slow effusive eruptions

Andrew W. Woods and Herbert E. Huppert

BP Institute and Institute for Theoretical Geophysics, Cambridge, UK

Received 6 June 2002; revised 18 October 2002; accepted 11 March 2003; published 29 August 2003.

[1] We explore some of the controls on the evolution of a slow effusive eruption imposed by processes in a shallow magma reservoir. We envisage that the emplacement of basaltic magma into a shallow, evolved crustal reservoir generates sufficient overpressure to trigger the slow effusive eruption of the overlying layer of evolved magma. The subsequent evolution of the system then depends on a number of factors including (1) the volatile contents of the two magmas; (2) the rate of any continuing influx of basalt; (3) the cooling/heating rates of the two layers of magma; and (4) the eruption rate of the silicic magma, where we assume that the crystals and bubbles remain in the layer in which they formed. Any exsolved volatiles in the magma increase the compressibility of the magma. In a waning system, this tends to increase the volume of material, which needs to be erupted to relieve a given overpressure by an amount of order 10–100, and hence increases the duration of the eruption. Typical calculations suggest that eruptions from magma chambers of size 1–10 km<sup>3</sup> may persist for times of order 1–10 years if the main body of silicic magma is saturated in volatiles. In addition, cooling of the basalt leads to formation of dense crystals, which lowers the pressure. However, if the magma becomes saturated, exsolution of volatile gases occurs, tending to increase the pressure. Again, in a waning system, this tends to extend the eruption duration and increase the mass erupted from the chamber. For chamber volumes of 1–10 km<sup>3</sup>, cooling rates of 10<sup>−6</sup> K/s can increase the eruption volume by a factor of order 10. Rapid cooling may also lead to an initial increase in the eruption rate, while the chamber pressure is controlled by the rate of production of new bubbles. If there is an influx of basalt to the chamber which is maintained during the eruption, then the evolution of the eruption is primarily dependent on this input rate, although the cooling of the basalt may increase the eruption rate to values in excess of this input rate, especially at an early stage in the eruption. The complex and nonlinear evolution of the eruption rate predicted by our simple model illustrates the sensitivity of the eruption rate to the magma volatile content and magma cooling rates. Such understanding is key in developing quantitative models for hazard assessments of slow effusive eruptions. *INDEX TERMS*: 8414 Volcanology: Eruption mechanisms; 8419 Volcanology: Eruption monitoring (7280); 8434 Volcanology: Magma migration; 8439 Volcanology: Physics and chemistry of magma bodies; *KEYWORDS*: effusive eruption, magma chamber, compressible, volatiles

**Citation:** Woods, A. W., and H. E. Huppert, On magma chamber evolution during slow effusive eruptions, *J. Geophys. Res.*, 108(B8), 2403, doi:10.1029/2002JB002019, 2003.

### 1. Introduction

[2] There has been much interest in the evolution of slow effusive eruptions from evolved magmatic systems following the injection of fresh basaltic magma. Notable eruptions include the 1991–1995 eruption of Mount Unzen in Japan, which exhibited some complex eruption cycles and the ongoing eruption of Soufriere Hills volcano, Montserrat, in which the effusion rate has averaged about 3–4 m<sup>3</sup>/s since the eruption commenced in 1995, even though there have been many complex shorter-term fluctuations (Figure 1) [Sparks *et al.*, 1998]. In attempts to understand these eruptions, much attention has focused on the evolution of

the flow in the conduit, leading to new models of the transitions in eruption regime driven by magma-gas separation and crystallization in the conduit [Jaupart and Allegre, 1991; Woods and Koyaguchi, 1994; Melnik and Sparks, 1999]. Here we develop a series of complementary models to examine the evolution of the magma reservoir during such slow effusive eruptions.

[3] In our model, we assume that the eruption is triggered by the intrusion of dense basaltic magma at the base of an evolved and relatively cold layer of more viscous silicic magma. We examine the subsequent evolution of the chamber under the competing effects of (1) the slow effusive eruption of magma from the upper layer, which tends to lower the chamber pressure [Wadge, 1978; Druitt and Sparks, 1984; Stasuiik *et al.*, 1993]; (2) the cooling of the fresh basaltic magma, which leads to formation of dense

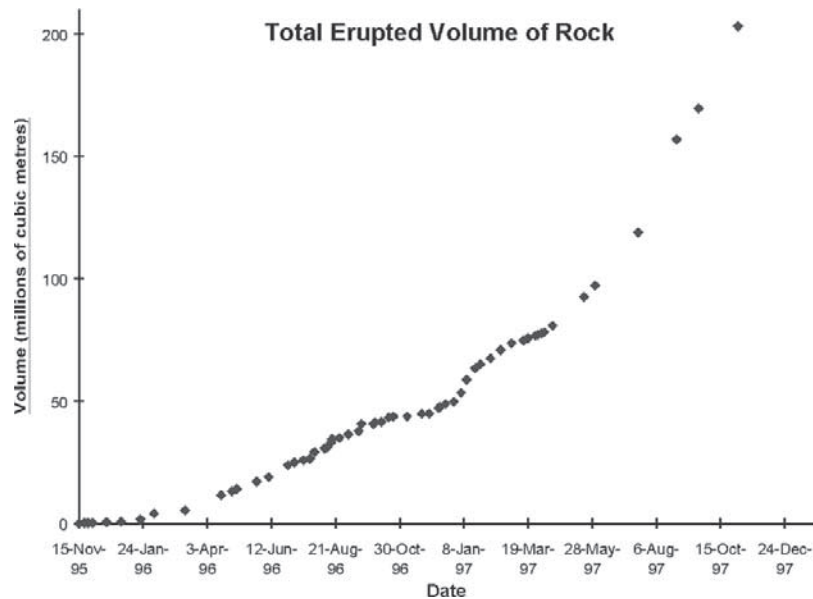


**Figure 1.** Progressive increase in the eruption rate during the 1994–1998 eruption of Soufriere Hills Volcano, Montserrat, British West Indies [after *Sparks et al.*, 1998].

crystals and, in a volatile unsaturated magma, a decrease in pressure, whereas for a volatile saturated magma, it leads to bubble formation and an increase in pressure [*Sparks et al.*, 1977; *Blake*, 1984; *Tait et al.*, 1989; *Woods and Pyle*, 1997; *Folch and Marti*, 1998]; (3) the heating of the crystalline silicic magma, which leads to dissolution of dense crystals and either a pressure increase in a volatile unsaturated magma, or associated resorption of volatile bubbles and a pressure decrease in a volatile saturated magma; and (4) the continued supply of basaltic magma to the chamber which tends to increase the chamber pressure.

[4] In previous models, it has been assumed that the magma chamber is either (1) closed and the effects of cooling and crystallization have been examined [*Tait et al.*, 1989; *Woods and Pyle*, 1997] or (2) open, with the pressure in the chamber evolving only as a result of inflow and outflow [*Stasuik et al.*, 1993; *Melnik and Sparks*, 1999]. However, in some slow effusive eruptions, the timescale for pressurization through cooling and crystallization may well be comparable to the timescale for decompression through eruption and recompression due to the continuing input of basalt into the chamber. The object of the present work is to illustrate the competition between these different influences on the chamber pressure and their impact on the ensuing effusive eruption. Many of the detailed properties of (1) the magma, especially the rheology and crystallization sequence, and (2) the chamber and conduit geometry, and associated strength of the surrounding crust, will vary from case to case and are not fully understood. Therefore we develop a simplified model which focusses on some of the key physical processes to provide insight into the underlying physical controls on eruption rate. Even with this simple model, our calculations illustrate how complex variations in eruption rate may be caused by the combination of the initial release of chamber overpressure, cooling-driven pressurization, and the continuing recharge of the chamber with new magma.

[5] In section 2 we introduce the key features of the model and derive a generalized equation governing the

temporal pressure variation in the chamber. Then we examine a series of model calculations of increasing complexity. Section 3 describes the evolution of the chamber pressure in the limit in which both the basaltic and silicic magmas are volatile free. This provides a reference with which we can interpret the effect of volatiles exsolved in the chamber on the eruption evolution, as is described in section 4. In section 5, we include the effects of cooling of the basalt on the evolution of the chamber pressure and hence eruption. We identify key differences between the cases in which the basalt layer and the silicic layer are saturated or under-saturated in volatiles. In each situation, we examine two end-member models for the evolution. First, we examine the case in which a finite mass of basalt is emplaced in the chamber prior to eruption, with no further input of basalt. Second, we explore the case in which there is a steady continuing input of basalt into the chamber from depth during the eruption, as may be the case during eruptions such as Soufriere Hills volcano, Montserrat.

## 2. The Model

[6] We consider the system shown in Figure 2, in which a layer of hot, volatile-rich basalt is emplaced beneath a crystalline layer of evolved silicic magma. We assume that after a finite mass of basaltic magma has been emplaced, the overpressuring of the crustal walls to the chamber drives a fracture to the surface, initiating an effusive eruption of the silicic magma. The details of the establishment of the conduit and the subsequent effusive conduit flow [*Stasuik et al.*, 1993; *Jaupart and Allegre*, 1991; *Woods and Koyaguchi*, 1994; *Melnik and Sparks*, 1999] may be complex, owing to changes in the rheology and density of the magma as it ascends to the surface. In order to focus on the chamber evolution, as a simplification we assume that the conduit has a fixed geometry, and that the silicic magma rises as a slow viscous flow at a rate proportional to the chamber overpressure, as described

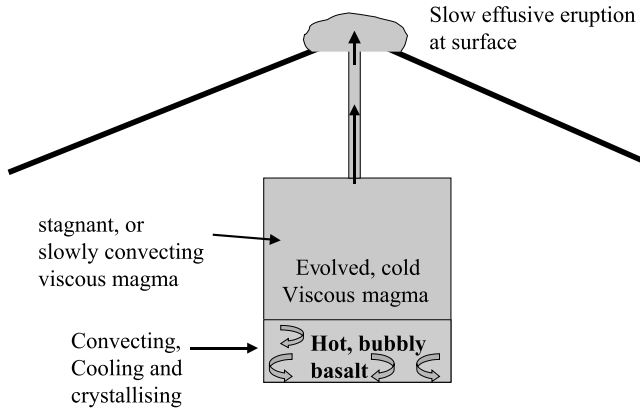


**Figure 2.** Schematic of a two-layered magma reservoir in which the upper viscous magma erupts effusively at the surface, driven by the emplacement, and subsequent crystallization and cooling, of the lower layer of dense, basaltic magma. Crystals and bubbles are assumed to remain in the layer of origin.

by Stasuiik *et al.* [1993]. Recent modeling work [Melnik and Sparks, 1999; Barmin *et al.*, 2002] has identified that complex, multiple conduit flow regimes may develop for a certain range of chamber pressures. With a chamber which is being steadily recharged, this can lead to complex eruption cycles. However, if the eruption continues for many such cycles, then the mean eruption rate over a cycle will match the mean input rate to the chamber plus any additional effects due to a change in the mass stored in the chamber, resulting for example from cooling and crystallization. In this way, it is the evolution of the magma reservoir and deeper source of magma which ultimately controls the long-term evolution of the eruption.

[7] In order to model the evolution of the chamber pressure, and its relation to the eruption, we present a model for the density of the magma-volatile mixture in the chamber, which depends on the pressure and temperature of the layer. We then combine this with a model of the pressure-volume evolution of the chamber, accounting for input and output of magma, and also deformation of the walls of the chamber as the pressure of the system evolves. Finally, we introduce a model for the thermal evolution of the system. The thermal evolution is important because as the lower layer of basalt cools it forms relatively dense anhydrous crystals, which tend to lower the chamber pressure. However, the dissolved volatiles in the melt eventually become saturated and are then exsolved on continued cooling, thereby leading to an expansion and repressurization of the system [Huppert *et al.*, 1982; Tait *et al.*, 1989]. In this model, we follow Huppert *et al.* [1982] and assume that the bubbles and crystals remain well mixed within the layer in which they form. We also assume that the exsolution of gas follows the equilibrium solubility relation, so that thermodynamic and chemical equilibrium is maintained between the phases. This is expected to be a very good approximation for the slow effusive eruptions examined in this work.

[8] We introduce simplified models for the density of the basaltic and silicic magmas, assuming that water is the volatile phase. We denote the mass fraction of crystals in

the magma  $i$  as  $x_i$ , where  $i = b$  and  $i = s$  correspond to the basaltic and silicic magmas respectively. We also assume that the mass fraction of water in solution in the melt phase is given by the saturation value [Sparks, 1978]

$$n_{is} = s_i p^{1/2}, \quad (1)$$

where  $p$  is the pressure and the saturation constant,  $s_i$ , has representative values  $s_b = 3 \times 10^{-6} \text{ Pa}^{-1/2}$  for basalt and  $s_s = 4 \times 10^{-6} \text{ Pa}^{-1/2}$  for silicic magma [Holloway and Carroll, 1994]. These values are used for convenience to provide qualitative understanding of the evolution of the volatile budget as the chamber pressure evolves, although we should beware that the quantitative details may vary for specific magmas. The mass fraction of exsolved volatiles  $n_i$  in layer  $i$  is therefore given by

$$n_i = N_i - n_{is}(1 - x_i), \quad (2)$$

where  $N_i$  is the total mass fraction of volatiles in magma  $i$ . The bulk density of this bubbly, crystal-laden basaltic magma,  $\rho_i$ , is given by

$$\rho_i = \left( \frac{n_i}{\rho_g} + \frac{1 - n_i}{\sigma_i} \right)^{-1}, \quad (3)$$

where  $\sigma_i$  denotes the bulk density of the mixture of magma  $i$  and its crystals. This is given in terms of the mass fraction of crystals in the melt,  $x_i$ , the density of the crystals,  $\sigma_c$  and the density of the melt phase of magma  $i$ ,  $\sigma_{mi}$ , according to the relation

$$\sigma_i = \left( \frac{x_i}{\sigma_c} + \frac{1 - x_i}{\sigma_{mi}} \right)^{-1} \quad (4)$$

The density of crystals depends on the mineral precipitated, but we take a typical value of  $2800 \text{ kg/m}^3$  for crystals precipitated from basalt and  $2600 \text{ kg/m}^3$  for crystals precipitated from silicic magma, while we assume the basaltic melt density has value  $\sigma_{mb} = 2600 \text{ kg/m}^3$  and the silicic melt density has value  $\sigma_{ms} = 2300 \text{ kg/m}^3$ . We approximate the density of the gas,  $\rho_g$ , which we assume is primarily composed of water vapor, by the perfect gas law

$$\rho_g = p/RT, \quad (5)$$

which is valid for shallow crustal pressures [Tait *et al.*, 1989]. Here  $R$  is the gas constant, with value  $462 \text{ J kg}^{-1} \text{ K}^{-1}$  for water vapor, and  $T$  is the basaltic temperature, measured in kelvins.

[9] In order to model the pressure response of the system to either a change in mass or the exsolution of gas, we account for the compressibility of the wall rock, the liquid magma, crystals and the exsolved gas bubbles. The gas bubbles are much more compressible than the liquid magma, crystals or the country rock. This may be seen from equation (5) in which the bulk modulus of the gas, which is inversely proportional to compressibility, has value of order  $p \sim 10^8$  Pa. This is 100–1000 times smaller than the bulk modulus of the magma,  $\beta \sim 10^{10} - 10^{11} \text{ Pa}$  [Touloukian *et al.*, 1981]. On compression of the system, the gas volume therefore

changes by a much greater fraction than the magma. However, the gas only occupies a small fraction of the total volume and so the total change in volume of the system depends on the volume of gas and volume of magma present. If the volume fraction of gas in the chamber exceeds the ratio of the compressibility of the gas to that of the magma, then the total change in volume will be greater than that of the magma alone [cf. *Bower and Woods*, 1997]. In this case, the layers of bubble-rich basaltic and silicic magma are able to sustain relatively large changes in volume for a given change in pressure, in comparison to the surrounding country rock. However, for smaller gas volumes, the compressibility of the liquid magma dominates that of the gas. In that case, the change in volume associated with the rock compressibility provides a lower bound on the erupted volume and hence time for the system to relax to equilibrium. We illustrate this in section 3.

[10] If the total mass of basaltic and silicic magma at any time  $t$  are denoted by  $M_b(t)$  and  $M_s(t)$ , and they occupy volumes  $V_b$  and  $V_s$ , then we can write the bulk densities of the basaltic and silicic magmas as

$$\rho_b = M_b/V_b, \quad \rho_s = M_s/V_s. \quad (6)$$

[11] If the wall rock surrounding the chamber is modeled as an elastic medium, then any change in pressure,  $dp$ , results in a change in volume given by [*Blake*, 1984]

$$dV = Vdp/\beta_w, \quad (7)$$

where  $\beta_w$  is the bulk modulus of the wall rock and  $V$  is the volume of the chamber. The magma within the chamber typically has different bulk compressibility compared to the country rock. Therefore either (1) the magma needs to undergo a phase change through cooling which causes a change in density or (2) there needs to be addition or removal of mass from the chamber, in order to balance both the changes in pressure and volume of the chamber, which are coupled through the deformation of the country rock according to equation (7). More complex equations than equation (7) exist relating the pressure with the change in chamber volume [*Timoshenko and Goodier*, 1970], but relation (7) captures the key physical balance, through the bulk viscosity, as shown by *Tait et al.* [1989]. The density of the liquid magma  $i$  varies with pressure according to the relation

$$d\sigma_i = -\sigma_i dp/\beta_i, \quad (8)$$

where  $\beta_i$  are the bulk moduli of the magmas. Here, we take this to be the same for the basaltic and silicic magmas, with value  $\beta_s = \beta_b = 10^{10}$  Pa. We also assume the bulk modulus of the country rock has value  $\beta_w \sim 10^{11}$  Pa. Note that although these are representative, the precise values depend on the specific location and properties of the rocks [*Touloukian et al.*, 1981].

[12] Combining equations (1)–(8), we can find an expression which relates pressure and volume changes in the chamber. This has the form

$$f \frac{dp}{dt} = \left[ \frac{Q_I}{\rho_b} - \frac{Q_O}{\rho_s} \right] + g_b \frac{dT_b}{dt} + g_s \frac{dT_s}{dt}, \quad (9)$$

where  $Q_I$  and  $Q_O$  are the rates of mass input and output from the chamber. The terms on the right hand side of equation (9) represent the rate of change of the volume resulting from (1) the output and input of material into the chamber (the first two terms) and (2) the temperature evolution of the layers of basaltic (third term) and silicic (fourth term) magma. We may interpret equation (9) as a generalized form of equation (7), where  $f$  has the interpretation of being the effective chamber volume divided by the effective compressibility of the magma in the chamber and the surrounding rock. In fact,  $f$  may be written as the sum of three distinct elements,

$$f = f_b + f_s + f_w, \quad (10)$$

where  $f_b$  and  $f_s$  may be interpreted as the volume of the basaltic and silicic magmas, divided by their respective bulk moduli

$$f_b = M_b \left( \frac{s_b(1-x_b)}{2p^{1/2}} \left[ \frac{RT}{p} - \frac{1}{\sigma_b} \right] + \frac{n_b RT}{p^2} + \frac{1-n_b}{\sigma_b \beta_b} \right) \quad (11)$$

$$f_s = M_s \left( \frac{s_s(1-x_s)}{2p^{1/2}} \left[ \frac{RT}{p} - \frac{1}{\sigma_s} \right] + \frac{n_s RT}{p^2} + \frac{1-n_s}{\sigma_s \beta_s} \right), \quad (12)$$

while  $f_w$  denotes the volume of the chamber divided by the bulk modulus of the surrounding wall rock

$$f_w = \frac{V}{\beta_w}. \quad (13)$$

The above expressions for  $f_b$  and  $f_s$  correspond to the situation in which the magma is saturated in volatiles. If the pressure of the system is larger, or the total volatile content is smaller, then there will be no exsolved volatiles in the magma, and the expressions reduce to [cf. *Blake*, 1984]  $f_b = M_b/(\sigma_b \beta_m)$  and  $f_s = M_s/(\sigma_s \beta_m)$ .

[13] The quantities  $g_b$  and  $g_s$  represent the rate of change of volume of the basaltic and the silicic magmas with temperature, again in the case that the magma is saturated in volatiles and includes an exsolved gas phase. The quantities are given by

$$g_b = M_b \left[ \frac{n_b R}{p} - n_{bs} \Gamma_b \left( \frac{RT_b}{p} - \frac{1}{\sigma_b} \right) - (1-n_b) \Gamma_b \left( \frac{1}{\sigma_c} - \frac{1}{\sigma_b} \right) \right] \quad (14)$$

$$g_s = M_s \left[ \frac{n_s R}{p} - n_{ss} \Gamma_s \left( \frac{RT_s}{p} - \frac{1}{\sigma_s} \right) - (1-n_s) \Gamma_s \left( \frac{1}{\sigma_c} - \frac{1}{\sigma_s} \right) \right], \quad (15)$$

where, for convenience, we have introduced the notation

$$\Gamma_i = -dx_i/dT. \quad (16)$$

to denote the rate of crystallization per degree of cooling in the basaltic and silicic magmas. The three terms on the right-hand side of equations (14) and (15) account for the change of gas volume with temperature, the production of new gas

associated with crystallization and the change in density of the crystals relative to the melt. We neglect the thermal expansion of the magma as this is dwarfed by the change in density associated with crystallization [cf. *Huppert et al.*, 1982]. For typical conditions, the dissolved gas contents,  $n_s$  and  $n_b$ , have values of order 0.01–0.04, while the rate of crystallization with cooling,  $-dx_p/dT$ ,  $-dx_s/dT = \Gamma_s$ ,  $\Gamma_b \sim 0.005^\circ\text{C}^{-1}$  [*Huppert and Sparks*, 1988]. The expressions for  $g_i$  illustrate that in a volatile unsaturated magma, the formation of relatively dense crystals on cooling tends to increase the bulk density. However, in a volatile saturated magma, the exsolution of volatiles associated with crystallization dominates the evolution of density, and leads to a decrease in density with cooling [cf. *Huppert et al.*, 1982; *Tait et al.*, 1989; *Woods and Pyle*, 1997]. Similarly, if the silicic magma is volatile unsaturated, then as it is heated up, some crystals are dissolved, and the volume tends to increase. However, if it is volatile saturated, then the volume of silicic magma tends to decrease as its temperature increases, primarily owing to the resorption of volatiles into the melt associated with the dissolution of anhydrous crystals. We explore the key role of volatiles in determining the pressure evolution of the system in section 5.

[14] We deduce from equation (9) that the chamber volume and hence pressure may either increase or decrease depending on (1) the rate of eruption compared to (2) the rate of cooling of the basalt or heating of the silicic magma, and (3) the magma recharge rate. The critical condition, under which the chamber pressure will remain constant is given by setting the right-hand side of equation (9) to equal zero, leading to the relation

$$g_b \frac{dT_b}{dt} + g_s \frac{dT_s}{dt} = \frac{Q_o}{\rho_s} - \frac{Q_r}{\rho_b}. \quad (17)$$

In order to satisfy equation (17) two situations may arise. For a system which erupts after a finite input of basalt and with no continuing input of basalt, the net pressurization associated with the heat transfer between the basaltic and silicic magma is required to match the depressurization associated with the eruption. If the silicic magma is erupting, then this may be a transient balance, with the system running down as more mass is erupted. However, for a system with a continuous input of basaltic magma, we might expect that, to leading order, the rate of eruption of the silicic magma will match the recharge rate of basaltic magma, so that the right-hand side of equation (17) by itself is approximately equal to zero. We explore this balance further in section 4. We delay discussion of the effects of heat transfer and temperature changes in the silicic and basaltic magmas until section 5. First we focus on the evolution of the chamber pressure which results from the input and output of magma, and explore the effects of exsolved volatiles in the chamber which increase the compressibility of the mixture [cf. *Bower and Woods*, 1997].

[15] To examine how the evolution of chamber pressure might influence the long-term eruption history, we require a model for the flow of silicic magma in the conduit to the surface. Field work and modeling of effusive eruptions of silicic magma has identified that during the slow ascent of silicic magma, exsolved volatiles can separate from the melt, as the magma develops a net permeability [*Eichelberger et al.*, 1986; *Jaupart and Allegre*, 1991; *Jaupart*, 1998; *Melnik*

and *Sparks*, 1999]. Although the detailed dynamics of the conduit flow are complex, the model predictions show that the eruption rate in as low effusive eruption gradually increases with pressure, up to a maximum flow rate at which there is a transition to a different eruption regime [*Woods and Koyaguchi*, 1993; *Melnik and Sparks*, 1999]. For the purpose of the present study, we can parameterize these results for the effusive eruption regime by adopting a model similar to that of *Stasuik et al.* [1993] in which the mass flow rate is assumed to increase with the overpressure,  $\Delta p$ , in the chamber, according to the simple law

$$Q_o = \frac{\rho_s S A^2 \Delta p}{\mu_s H} = \rho_s \gamma \Delta p, \quad (18)$$

where, for simplicity,  $\rho_s$  is taken to have the same value as in the chamber (equation (3)). Here  $S \sim 0.1$  is a shape factor,  $H$  denotes the depth of the chamber below the surface, taken to be 5 km in all the calculations in this paper (except for Figure 9 in section 5.3),  $A$  is the cross-sectional area of the conduit,  $\mu_s$  is the viscosity of the silicic magma, and the constant  $\gamma$  is defined by equation (18).

[16] In order to develop understanding of the chamber evolution, we now present a series of model calculations. First, we consider the case in which the silicic magma slowly erupts, with no cooling of the basalt or heating of the silicic magma, and no recharge of basaltic magma. We then examine the influence of a slow recharge of basaltic magma during the eruption. Next, we examine the potential role of cooling of the basalt on the evolution of the chamber pressure and hence the eruption rate, and compare the model calculations to the case with no cooling.

### 3. Eruption Evolution With No Exsolved Volatiles

[17] As a limiting case we examine the evolution of the magma chamber in the case in which the magmas remain under saturated to volatiles and there is no cooling of the basalt. This provides a reference with which we can assess the influence of any exsolved volatiles or heat transfer on the evolution of the eruption. In the limit of an under saturated magma, with no volatiles,  $f_s$  and  $f_b$  simplify to  $V_s/\beta_s$  and  $V_b/\beta_b$ . Therefore equation (9) reduces to the classical model [cf. *Blake*, 1981, equation 2.7]

$$\frac{dp}{dt} = \frac{\bar{\beta}}{V} \frac{dV}{dt}, \quad (19)$$

where  $V$  is the chamber volume, and the effective bulk compressibility is given by the geometric average of the magma compressibility and that of the country rock,  $\bar{\beta} = V(V_b/\beta_b + V_s/\beta_s + V/\beta_w)^{-1}$ . Equation (19) illustrates that the volume which needs to be erupted to release a chamber overpressure,  $\Delta p$ , is given by

$$\Delta V = V \Delta p / \bar{\beta}. \quad (20)$$

Eruption of only a very small fraction of the volume of the chamber, of order  $10^{-3}V$ , is required to relieve an initial overpressure of order 10 MPa [cf. *Blake*, 1981]. In slow effusive eruptions, with volume eruption rates of order 1.0–10.0 m<sup>3</sup>/s, the time for eruption will then be of order  $(10^{-4}$ –

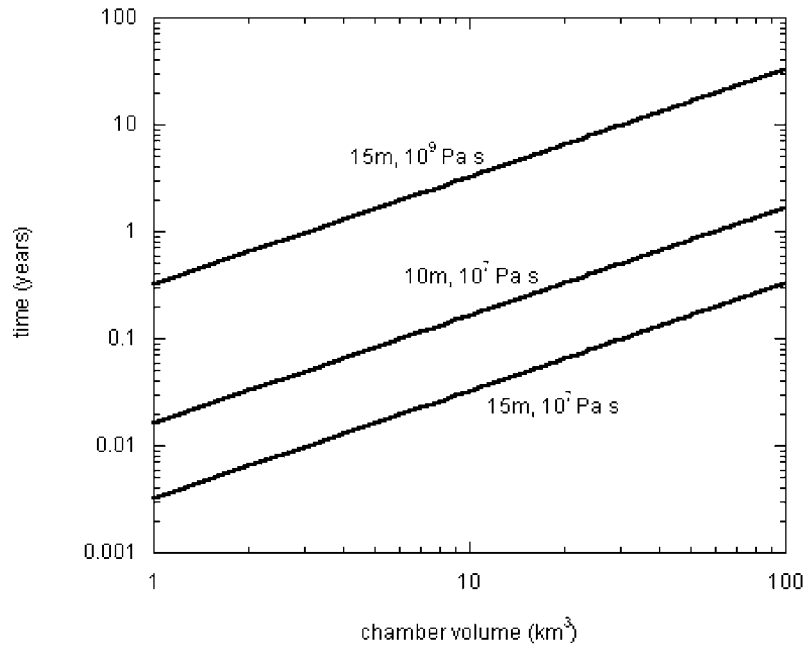


**Figure 3.** Timescale for eruption as a function of the chamber volume, for a chamber overpressure of 10 MPa. Curves are shown for three cases: case i, conduit radius of 15 m and magma viscosity  $10^7$  Pa s; case ii, conduit radius of 10 m and magma viscosity  $10^7$  Pa s; and case iii, conduit radius of 15 m and magma viscosity  $10^9$  Pa s.

$10^{-3})V$  s, where  $V$  is measured in  $\text{m}^3$ . If the volume of the chamber lies in the range  $0.1\text{--}100\text{ km}^3$ , then we anticipate eruption times of order  $10^4\text{--}10^8$  s, with the upper end of this range corresponding to a large chamber with a slow eruption rate [cf. Blake, 1981]. However, observations of a number of waning effusive eruptions suggest that they continue for several years [Stasuik et al., 1993], with typical volumes of erupted material in the range  $10^{-4}\text{--}10^{-1}\text{ km}^3$ . This volatile-free model of chamber evolution would therefore suggest that many historic eruptions are associated with large magma chambers, in excess of  $100\text{ km}^3$ . However, in sections 4 and 5 we identify that the much higher compressibility of any bubbles exsolved in the magma may lead to comparable erupted volumes from chambers which are 10–100 times smaller in volume.

[18] When a chamber is recharged with basaltic magma, the chamber pressure may build up until it attains a critical overpressure at which point it drives open a flow path to the surface. Subsequently, an effusive eruption can develop and the system will tend to evolve toward a steady balance between the recharge and the eruption, with the chamber pressure adjusting so that the input balances the output. This development may be described by combining equation (9) for the pressure evolution, with the conduit flow law (18), leading to (see equation (19))

$$V \frac{d\Delta p}{dt} = \bar{\beta} \left( \frac{Q_I}{\rho_b} - \frac{\lambda \Delta p}{\rho_s} \right) \quad (21)$$

for the overpressure of the chamber,  $\Delta p$ . Since typical pressure changes within a magma chamber are smaller than  $10^8$  Pa, and the erupted volume,  $\Delta V \sim (10^{-4}\text{--}10^{-3})V$ , then, in the expression on the left-hand side of equation (21), we

may approximate the volume of the chamber as being constant since the bulk modulus of the wall rock is of order  $10^{11}$  Pa. In this case, we can find a simple solution for equation (21). Indeed, if the overpressure at which the conduit breaks through to the surface and the eruption commences is  $\Delta p_o$ , then for a constant influx  $Q_I$ , equation (21) predicts that the subsequent evolution of the chamber overpressure is given by the relation

$$\Delta p(t) = \frac{Q_I}{\rho_b \gamma} + \left( \Delta p_o - \frac{Q_I}{\rho_b \gamma} \right) \exp(-\bar{\beta} \gamma t / V) \quad (22)$$

This involves a simple adjustment to a constant overpressure  $Q_I / \rho_b \gamma$  which is necessary to drive an outflow equal to the input to the chamber.

[19] The time scale for the adjustment,  $V / \gamma \bar{\beta}$ , varies with the chamber volume as well as the properties of the conduit, expressed in the parameter  $\gamma$  as given by equation (18). The conduit height is taken to be 5000 m. In Figure 3 we illustrate typical values for this time scale as a function of the chamber volume for three values of the conduit radius  $r$  and the silicic magma viscosity  $\mu_s$ : (1)  $r = 15$  m,  $\mu = 10^7$  Pa s; (2)  $r = 10$  m,  $\mu = 10^7$  Pa s; and (3)  $r = 15$  m,  $\mu = 10^9$  Pa s. On reaching the steady state, the chamber pressure would then change only if (1) the input flux evolved, (2) the geometry of the conduit to the surface varied with time, owing perhaps to thermal or mechanical erosion, or (3) the eruption rate to the surface changed owing to some more complex conduit flow dynamics [cf. Melnik and Sparks, 1999; Barmin et al., 2002].

[20] These models identify that for volatile unsaturated magma the eruption rate varies exponentially with time, until the chamber overpressure has adjusted to an equilib-

rium value in which the eruption rate equals the rate of input of basaltic magma. Owing to the highly incompressible nature of the rock, only a small fraction of the volume of the chamber, of order  $10^{-3}$  needs to erupt for the pressure to adjust, and so the timescale for this adjustment is of order days to months unless the chamber volume is in excess of about  $100 \text{ km}^3$ .

#### 4. Influence of Exsolved Volatiles in the Chamber

[21] We now examine how the presence of any exsolved volatiles in the chamber influences the results described in section 3. We consider two end-member models. First, the case in which a finite mass of basaltic magma is intruded into a chamber, prior to the onset of an eruption. Second, we examine the case in which there is a constant flux of basalt input to the chamber during the eruption of the silicic magma. In both cases we examine the sensitivity of the results to the mass of volatiles in both the silicic and the basaltic magmas, examining cases in which one or both layers are saturated.

[22] We anticipate that the volatile contents of both the basaltic and silicic magmas are important, because the volatiles can increase the compressibility of the system, thereby allowing a much larger volume of material to erupt for a given decrease in overpressure, and hence increasing the longevity of the eruption. Indeed, the relative importance of the compressibility of the bubbles may be deduced from the expressions for  $f$  (equations (10)–(13)). A comparison of the magnitude of the different terms indicates that for sufficient exsolved gas contents,  $n_b, n_s \sim 0.01$ , with a typical pressure  $p \sim 10^8 \text{ Pa}$ , and typical bulk moduli  $\beta_{i,w} \sim 10^{10}–10^{11} \text{ Pa}$ , then the compressibility of the bubbles is  $10^2–10^3$  larger than that of the melt.

[23] For the case of an eruption which is driven by the initial overpressure in the chamber, equations (9) and (18) may again be used to determine the evolution of the eruption. In this case we have

$$f \frac{d\Delta p}{dt} = -\gamma \Delta p, \quad (23)$$

where  $f$  is now a function of pressure, according to equation (2.10–2.13). As the chamber pressure decreases, the mass of silicic magma also decreases, as given by equation (18), in the form

$$\frac{dM_s}{dt} = -\rho_s \gamma \Delta p. \quad (24)$$

In Figure 4 we present the model predictions for the evolution of eruption rate and erupted volume for a series of different conditions in order to compare the effects of exsolved volatiles in the basaltic and silicic layers of magma, with the cases in which one or other of the layers of magma is volatile free. In interpreting Figure 4, it is worth reminding the reader that in our model, the eruption rate is directly proportional to the chamber overpressure. In our calculations, we assume that the initial chamber overpressure is  $10^7 \text{ Pa}$ , the silicic magma has viscosity  $10^7 \text{ Pa s}$ , the chamber volume is  $10 \text{ km}^3$  and initially contains a volume fraction of 0.1 of basaltic magma, and the conduit radius is 15 m. The increase in compressibility

associated with the volatiles leads to an increase in the volume erupted from the chamber by a factor of 10–100 compared to the volatile free case, and the duration of the eruption increases by a comparable amount. In Figure 4 we present four different cases to illustrate the importance of exsolved volatiles in case i the basaltic magma; case ii the silicic magma; and case iii both layers of magma, in comparison to case iv the case in which both layers are undersaturated in volatiles. For case i, we assume the basaltic magma has a total volatile mass fraction of 0.04, while the silicic magma is always undersaturated; for case ii we assume the basaltic magma is always undersaturated, while the silicic magma has a total volatile mass fraction 0.04; in case iii we assume the basalt has a volatile mass fraction 0.04 and the silicic has a volatile mass fraction 0.04. In each calculation, the silicic magma has a crystal mass fraction of 0.4, while the basalt is crystal free. The presence of volatiles in the silicic magma has the most significant effect on the results; in the specific calculations of Figure 4, it leads to eruption of about 16 times more material than for the case in which the silicic magma is volatile undersaturated (curves for cases ii and iv). Although the presence of volatiles in the lower layer of basaltic magma increases the erupted volume, it has a smaller influence on the eruption evolution since it represents a much smaller fraction of the total volume. For example, comparing the case of a volatile saturated and unsaturated layer of basaltic magma, with a volatile unsaturated layer of silicic magma, we find the eruption volume only increases by a factor of about 3.5 (curves for cases i and iv). The quantitative details for a specific situation clearly depend on the specific volatile content in each layer, the relative volume of each layer, and the values of the other physical parameters, but the general principles are captured by Figure 4.

[24] The calculations in Figure 4 illustrate that volcanic systems with relatively modest sized chambers, of order  $10 \text{ km}^3$ , may sustain an effusive eruption for times as long as one year, erupting volumes as large as  $2 \times 10^8 \text{ m}^3$ , primarily as a result of the presence of exsolved volatiles. In volatile under-saturated magma, the erupted volume may only be  $10^7 \text{ m}^3$  for a comparable sized chamber. For these calculations, the erupted volumes increase in proportion to the size of the chamber. The results suggest that if the magma is saturated in volatiles in the magma chamber, then predictions of chamber size, based on observations of eruption rate and duration, may be 10–100 times smaller than anticipated from the theory for which the magma is assumed unsaturated. Knowledge about the volatile saturation of magma in a subsurface reservoir may therefore be highly significant for the interpretation of geophysical data during effusive eruptions, especially if the size of the subsurface chamber can be estimated from ground deformation and other geophysical measurements.

[25] With a continuing input of basaltic magma to the chamber, equation (9) may again be used to describe the evolution of the chamber pressure, but now it takes the form

$$f \frac{d\Delta p}{dt} = -\gamma \Delta p + \frac{Q_I}{\rho_b} \quad (25)$$

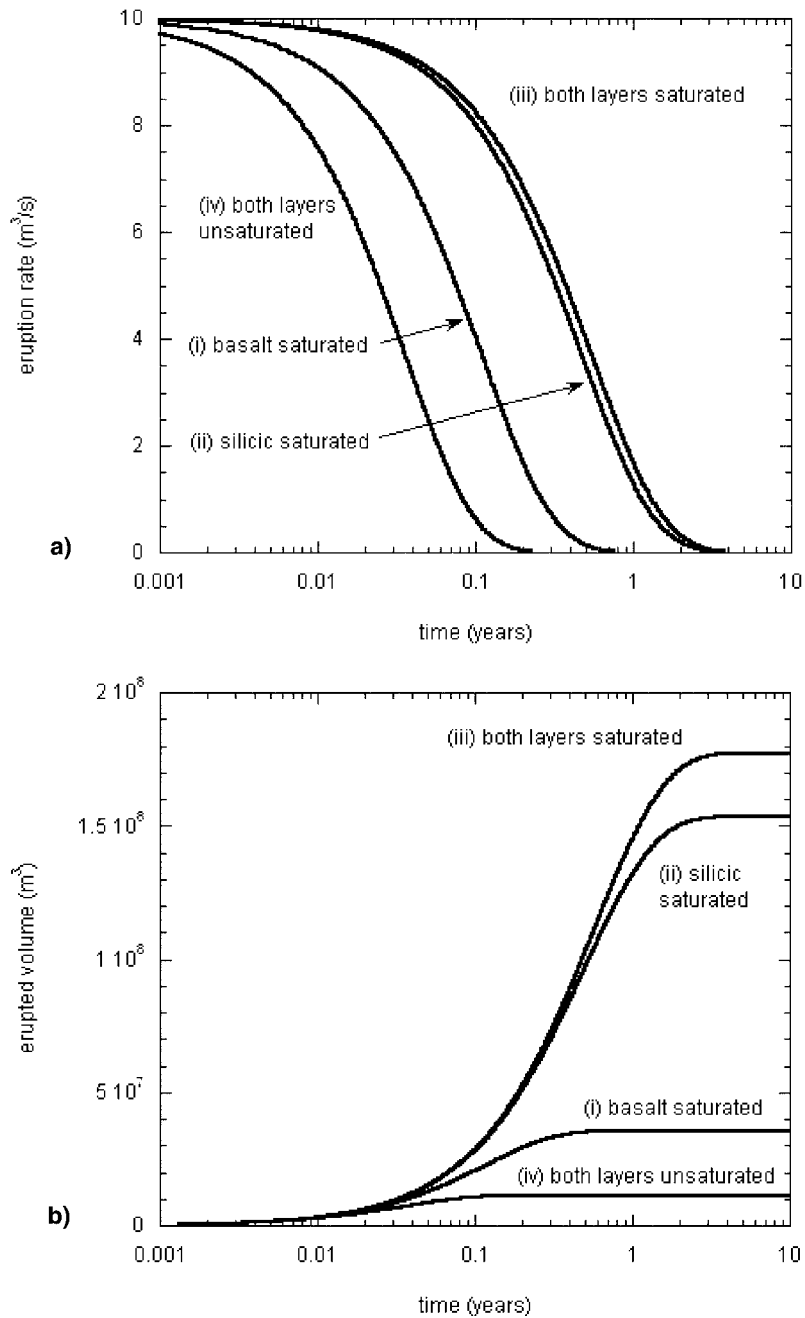


**Figure 4.** Evolution of (a) the volume eruption rate which is proportional to the chamber overpressure and b) the total erupted volume as functions of time, for four typical eruption conditions. Case i, the upper silicic layer remains volatile unsaturated, and the basaltic layer is volatile saturated, with a total water mass fraction of 4 wt %. The basalt has zero crystal mass fraction while the silicic magma has 40 wt % crystal mass; case ii, the upper silicic layer is volatile saturated, with a total mass fraction of water of 4 wt % and a mass fraction 0.4 of crystals, while the basalt remains undersaturated; case iii, both layers are volatile saturated, with the same initial volatile and crystal contents as used for the saturated layers in cases i and ii; and case iv, both layers are volatile unsaturated. In all calculations, the chamber is assumed to have a volume fraction 0.1 occupied by basaltic magma at the onset of the eruption, and no further input of basalt occurs. In these calculations, the chamber volume is taken to be  $10 \text{ km}^3$ . The magma is also assumed to remain isothermal, with the basalt temperature being  $1100^\circ\text{C}$  and the silicic temperature being  $800^\circ\text{C}$  during the eruption.

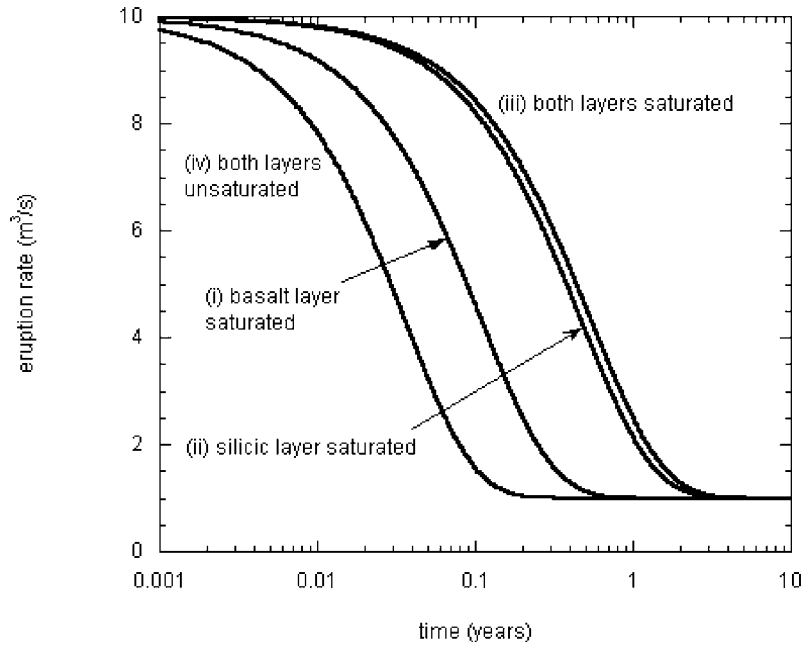


**Figure 5.** Variation in eruption rate as a function of time, for the same magmatic conditions as used in Figure 4, but now we include an input of basaltic magma at the base of the chamber, with a steady input rate of  $1 \text{ m}^3 \text{ s}^{-1}$ .

to account for both the input and output. The mass of silicic magma decreases during the eruption according to equation 4.2, while the mass of basaltic magma increases according to the relation

$$\frac{dM_b}{dt} = Q_I. \quad (26)$$

As for the case of volatile undersaturated magma, in this model the system converges toward a steady state in which the volume flux of the erupting silicic magma equal to the volume flux of incoming basaltic magma. In Figure 5 we present the results of some calculations of the possible evolution of the eruption rate with time for such a system, assuming an input rate of basaltic magma of  $1 \text{ m}^3 \text{ s}^{-1}$ . In Figure 5, the initial eruption rate, which is determined by the overpressure required to open up the flow path to the surface, is  $10 \text{ m}^3 \text{ s}^{-1}$ , according to the simple law (18). With a volatile saturated layer of silicic magma, the time required for the eruption rate to converge to the steady state value is considerably longer than in the case of a volatile poor magma (section 3), again owing to the much greater compressibility of magma containing exsolved volatiles. These volatiles tend to buffer the system in that more material needs to be erupted in order for the chamber pressure to evolve by a given amount and therefore converge to the steady eruption regime. As for the case of an instantaneous input, Figure 5 illustrates that the bulk compressibility of the system largely depends on whether the original layer of silicic magma is volatile saturated. This is because in our calculations the silicic magma represents the main mass in the chamber. If the silicic magma does contain a significant volume of exsolved volatiles, then the timescale for adjustment is nearly two

orders of magnitude greater than for the undersaturated silicic magma.

## 5. Effects of Cooling and Crystallization

[26] The calculations above illustrate how the system evolves with either a short-lived injection of basaltic magma or a maintained input. These calculations point to the crucial role that volatiles have in increasing the timescale of the eruption, and also the mass of material erupted, if there is an instantaneous input of basalt which invades the chamber. However, as well as input and output of magma to the chamber, the volatile budget in a chamber may evolve owing to any cooling and crystallization of the basalt and associated heat transfer to the silicic magma within the chamber [cf. *Tait et al.*, 1989; *Folch and Marti*, 1998]. Since effusive eruptions are relatively long-lived, with timescales of years to tens of years, then over the course of the eruption, there may be substantial cooling of any basalt injected into the chamber. This leads to crystallization of relatively dense minerals. While the basalt is volatile undersaturated, this causes an increase in density and therefore a decrease in chamber pressure. However, once the residual melt has become volatile saturated, the concomitant exsolution of water vapor repressurizes the system. Meanwhile, heat transferred from the cooling basalt to the overlying silicic magma leads to dissolution of some crystals. In a volatile unsaturated layer of silicic melt this causes an increase in pressure, whereas in a volatile saturated layer, the dissolution of crystals will lead to resorption of some volatiles and hence a decrease in pressure. We now explore these competing effects.

[27] *Tait et al.* [1989] and *Folch and Marti* [1998] have shown that in a closed magma chamber, with no input or

output, the pressure in the chamber may gradually increase owing to cooling, crystallization and exsolution of volatiles. Here, we assess the relative magnitude of this pressurization of the chamber, compared to the effects of the input and output of magma, on the chamber pressure. We present our model calculations in reference to the calculations of sections 3 and 4 in which we examined the chamber evolution in the absence of heat transfer.

[28] To include the effects of cooling in our model, we adopt the full equation for the evolution of the chamber pressure (equation (9))

$$f \frac{dp}{dt} = \left[ \frac{Q_I}{\rho_b} - \frac{Q_O}{\rho_s} \right] + g_b \frac{dT_b}{dt} + g_s \frac{dT_s}{dt}. \quad (27)$$

The new aspects of this model, in comparison with section 4, are the last two terms on the right-hand side of equation (27), which correspond to the rate of change of volume of the basaltic and silicic magmas as their temperatures evolve through heat transfer.

[29] In order to proceed, we require a model of the cooling of the basalt and the associated heating of the silicic magma. In the general case, for which (1) heat is transferred from the basalt to the upper layer of silicic magma with a heat flux  $F_c$ ; (2) heat is transferred from the basalt to the country rock with a heat flux  $F_b$ ; and (3) heat is transferred from the silicic magma to the country rock with heat flux  $F_s$ , then the conservation of heat in each layer of magma leads to two equations which govern the temperature evolution of the layers. The heat content of the basaltic layer decreases owing to the heat transferred to the silicic magma and country rock, while the input of new, hot basalt, with temperature  $T_i$ , into the chamber heats up this layer, according to the relation

$$M_b(C_p + L\Gamma_b) \frac{dT_b}{dt} = -F_c - F_b + (C_p + L\Gamma_b)Q_i(T_i - T_b). \quad (28)$$

Here  $C_p$  is the specific heat of the basaltic magma plus volatiles and  $L$  is the latent heat of crystallization. In contrast, the temperature of the silicic magma evolves according to the relation

$$M_s(C_p + L\Gamma_s) \frac{dT_s}{dt} = F_c - F_s, \quad (29)$$

where for convenience, we take the specific heats of the basaltic and silicic magmas to be equal.

[30] To complete the thermal model, we need to know the heat transfer relations  $F_c$ ,  $F_b$  and  $F_s$ .  $F_c$  depends on the intensity of any buoyant convection in either layer of magma [Turner, 1979; Huppert and Sparks, 1988]. In turn, this depends on the evolving rheology and density of the basaltic and silicic magmas, both of which are related to the bubble and crystal production rates [Cardoso and Woods, 1999]. The heat transferred to the silicic magma depends on whether the basalt is volatile saturated or undersaturated: in a saturated basalt any convection which develops in the basalt is driven at the lower boundary of the basalt by the production of relatively buoyant bubbles as basalt cools and

crystallizes [Cardoso and Woods, 1999]; in an undersaturated basalt, the convection is driven at the upper boundary of the basalt, owing to the formation of the relatively dense crystals. Many of these physical processes are still the subject of research, and detailed parameterizations which account for the different convective regimes are not available. In order to simplify the analysis, we therefore adopt a simple parametric model to examine the influence of the cooling of the basalt on the eruption history. For simplicity, we examine a range of representative values for the heat transfer from the basalt to the silicic magma,

$$F_c = (C_p + L\Gamma_b)GM_b, \quad (30)$$

where the parameterized cooling rate,  $G$ , typically lies in the range  $10^{-5}$ – $10^{-8}$  °C s<sup>-1</sup> for a 1–100 m thick sill (see Appendix A [Huppert and Sparks, 1988]). For the present study, in order to illustrate the potential impact of cooling on the evolution of the chamber pressure and the eruption rate, we assume that  $G$  is steady. We also neglect the heat transfer from the magma to the surrounding country rock; this simplification is valid for the case that the convection between the layers is the dominant mode of cooling of the basalt and implies that  $dT_s/dt = M_bG/M_s$ . In this model, we also assume that the crystals stay in the layer in which they were produced.

### 5.1. Evolution With Heat Transfer Only

[31] In the absence of any input or output of material from the chamber, the pressure of the closed system evolves according to the simple balance

$$f \frac{dp}{dt} = g_b \frac{dT_b}{dt} + g_s \frac{dT_s}{dt}, \quad (31)$$

where  $g_i$  are defined in section 2. Numerical solutions of this equation are shown in Figure 6 and illustrate how the pressure of the chamber evolves with time owing to the cooling and crystallization. For simplicity, in this and subsequent figures, we assume a linear relation between temperature and crystal content for both layers of magma, as parameterized by  $\Gamma_i = -dx_i/dT$ , as introduced in section 2. The basaltic magma is assumed to have initial temperature of 1100 K and  $\Gamma_b = 0.005$ , while the silicic magma has a temperature 800 K with  $\Gamma_s = 0.005$  [cf. Huppert and Sparks, 1988]. We also assume that initially the silicic magma occupies 90% of the chamber volume. Curves are given for four different configurations, corresponding to the cases introduced in Figure 4.

[32] In case i, the silicic magma remains volatile unsaturated, while the basalt is assumed to be volatile saturated, with the total mass fraction of volatiles in the basalt being 4 wt %. The cooling rate of the basalt,  $G$  (equation (30)) has value  $10^{-6}$  K s<sup>-1</sup>, in which case the basaltic sill requires several tens of years to cool and crystallize (Figure 6). As heat is transferred from the basaltic to the silicic magma, the chamber pressure increases very rapidly in response to the exsolution of volatiles in the basalt. The fast build up of pressure occurs because of two effects. First, with the silicic magma unsaturated in volatiles, the bulk compressibility of the system is much larger. Secondly, the unsaturated silicic magma expands as it is heated and resorbs crystals.

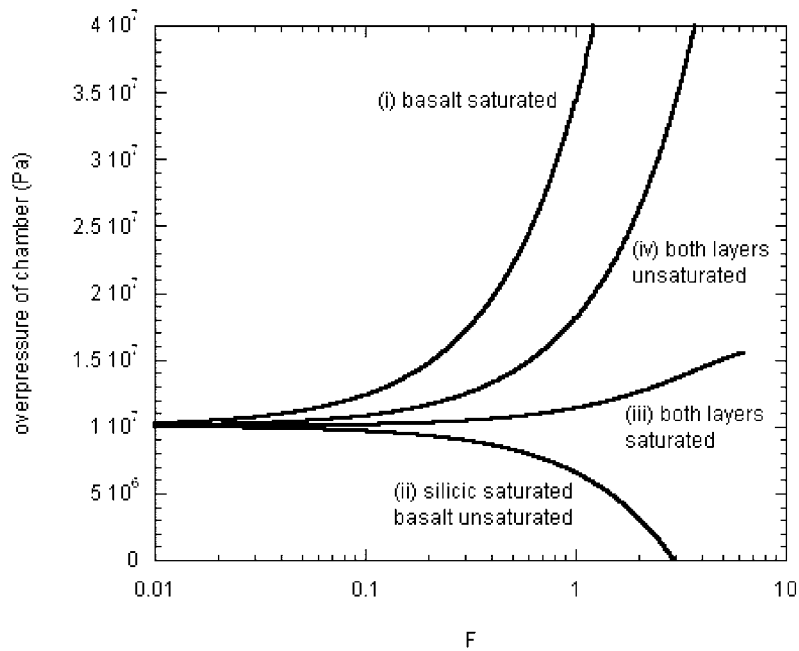


**Figure 6.** Evolution of the overpressure in the chamber as a function of the cooling rate of the basaltic magma, assuming that there is no input and no eruption of material from the chamber. The curves correspond to the four magma configurations of Figure 4, with a basaltic cooling rate of  $10^{-6} \text{ K s}^{-1}$  and all the heat released being transferred to the silicic magma. The basalt is assumed to have initial temperature  $1100^\circ\text{C}$ , and the silicic magma has initial temperature  $800^\circ\text{C}$ .

[33] In case ii, the basaltic layer is taken to be volatile unsaturated, while the silicic layer is volatile saturated, with a total of 4 wt % volatiles. The cooling rate is as in case i. Now the volatile unsaturated basalt contracts as it cools and crystallizes relatively dense crystals. However, the silicic magma also contracts as it is heated up owing to the resorption of gas as crystals are redissolved into the melt phase. The combination of these effects leads to a pressure decrease in the chamber.

[34] In case iii both layers are volatile saturated, with the total mass fraction of volatiles in the basalt being 4 wt % and in the silicic magma being 4 wt %. The cooling rate is as in case i. In this calculation, the chamber pressure increases owing to the increasing volume of the basalt as it cools, crystallizes and exsolves gas. However, the increase in pressure is relatively small since it is largely accommodated by the compression of the existing gas in the much larger silicic layer, and some resorption of the gas in the silicic layer as it is heated and redissolves crystals.

[35] In case iv, both layers are assumed to be volatile unsaturated, so that the basalt tends to contract on cooling, while the silicic magma expands as it is heated and resorbs crystals. The volume increase as dense crystals are resorbed into the silicic magma is greater than the volume decrease associated with growth of dense crystals in the basaltic magma. As a result, the model predicts an increase in pressure with time. Furthermore, since there is no gas in the system in this case, the bulk compressibility of the system is small, and rate of pressurization is large.

[36] By comparison with the results of sections 2–4 (e.g., Figure 4) we deduce that for cooling rates of order  $10^{-6} \text{ K s}^{-1}$ ,

the timescale and magnitude of the pressurization or depressurization due to heat exchange between the basaltic and silicic magmas may be comparable to that associated with the eruption from and input of mass into the chamber. We now examine how these different processes may interact.

## 5.2. Evolution With Heat Transfer and Slow Effusive Eruption

[37] First, we consider a system which is erupting material, with no further input of magma into the chamber. As in section 4, we assume the basalt initially occupies 10% of the volume of the chamber. Figure 7 illustrates how the eruption rate evolves with time assuming that the convective heat flux from the basaltic magma has parameterized cooling rate  $G$  (equation (30)) equal to  $10^{-6} \text{ K s}^{-1}$ . The four cases correspond to the four chamber configurations used in Figure 6 above.

[38] If the silicic magma is unsaturated while the basalt is volatile saturated (case i), the bulk compressibility of the system is relatively small, and so the pressurization of the system associated with volatile exsolution in the basalt is largely accommodated through eruption of the relatively incompressible silicic magma. The continual heating of the silicic magma leads to resorption of dense crystals and serves to enhance this pressurization of the chamber. As a result, after a few years, this configuration displays the largest eruption rate.

[39] In the case of an unsaturated basalt and a saturated silicic magma (case ii), the pressure of the system decreases both in response to the eruption of material from the chamber and also as heat is transferred from the basaltic

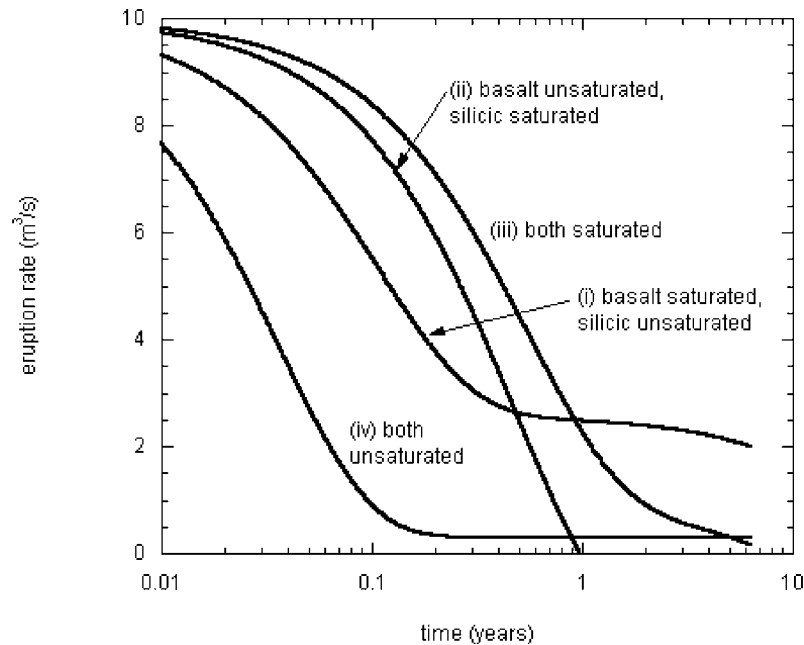


**Figure 7.** Eruption rate as a function of time, as for the conditions of Figure 4, but allowing for heat transfer between the basaltic and silicic melts. Curves showing the evolution of the erupted volume and the eruption rate up to the time that the layer of basalt has cooled to the solidus temperature of 900°C.

to the silicic magma. In this case, the eruption is very short lived before the excess chamber pressure has fallen to zero.

[40] If both layers of magma are volatile saturated (case iii), then owing to the relatively large compressibility, the pressure and hence eruption rate evolve relatively slowly. As a result, the eruption rate wanes rather slowly. In contrast, if both layers are volatile unsaturated, then the system is highly incompressible. In a closed system, this leads to a rapid pressure increase as the bulk density of the magmas decrease (Figure 6). However, with eruption of material, the chamber pressure evolves very rapidly until reaching a balance between (1) the net pressurization associated with the dissolution of dense crystals in the silicic magma and the formation of dense crystals in the basaltic magma, and (2) the pressure decrease associated with the eruption of material.

[41] With both layers of magma remaining unsaturated (case iv), the chamber is relatively incompressible, and the eruption rate adjusts rapidly to match the net rate of expansion of the magmas as the basalt crystallizes and the silicic magma resorbs crystals owing to the heat transfer.

### 5.3. Evolution With Input, Output, and Heat Transfer

[42] In Figure 8, we examine the effect of a maintained input of basalt to the system in addition to the cooling and eruption of silicic magma. For reference, calculations are shown for each of the four cases presented in Figures 6 and 7. The results are very similar to the results shown in Figure 7, in which there is no input to the chamber, except that the input of new material to the chamber leads to elevated eruption rates.

[43] In the calculations presented above, we have assumed that the layers of magma are either volatile saturated or unsaturated throughout the eruption. However,

it is possible that initially the basalt is unsaturated but that as it cools, it attains a critical crystal content at which it becomes saturated. In this case, the rate of pressurization of the system associated with the cooling, will evolve rapidly as the basalt begins to exsolve volatiles. To illustrate this effect, Figure 9a compares the results of three calculations, corresponding to a volatile saturated silicic layer with a total of 4 wt % volatiles overlying a basaltic layer of different initial volatile content: First, for reference, we present a basaltic layer, with a total of 4 wt % volatiles. In this case, the basalt remains volatile saturated through the eruption period, as in Figure 8. Then we illustrate the evolution of a basaltic magma with a total of 3 wt % water (Figure 9a). This layer only becomes volatile saturated after about 0.8 year. Before this time, the system behaves as the case considered in Figure 8 in which the silicic layer is volatile saturated while the basalt is unsaturated, but after about 0.8 year, the basalt exsolves volatiles, the system pressure is maintained, and the eruption rate wanes much more slowly. Finally, we illustrate the evolution of a basaltic magma with 2 wt % water which does not become volatile saturated, leading to termination of the eruption after about 1.4 years.

[44] Figure 9b illustrates the variation of eruption evolution with time for chambers at different depths in the crust. In each case, the basaltic and silicic magmas both have total volatile contents of 4 wt % and are volatile saturated, as for the case presented in Figure 8. Figure 9b illustrates that for the chamber 7.5 km below the surface, the gradual heating of the upper layer and associated resorption of crystals and volatile bubbles eventually causes the upper layer to become unsaturated. Beyond this time, the bulk compressibility of the system is much smaller, and so any further cooling and crystallization of the basalt leads to a sharp

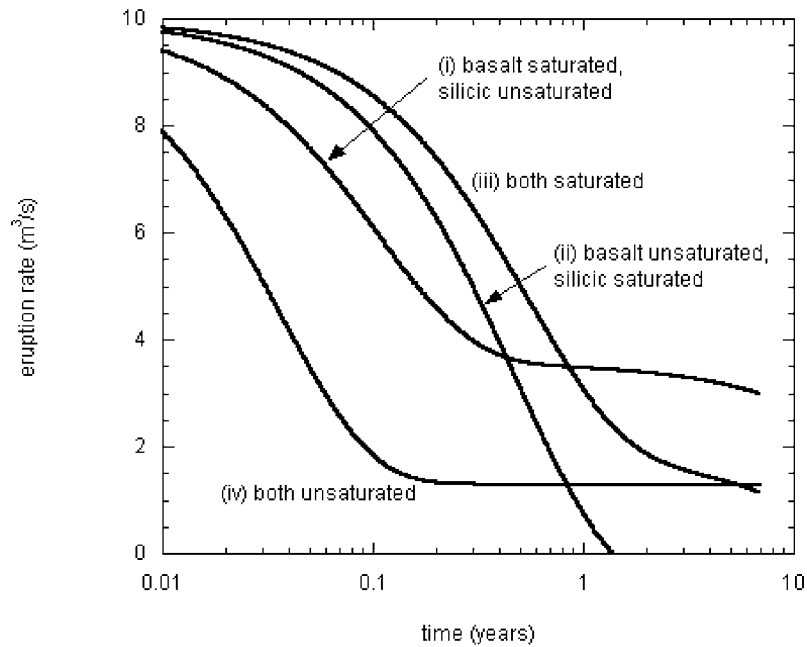


**Figure 8.** Variation in eruption rate with time for the same conditions as in Figure 7, but with a magmatic input of  $1 \text{ m}^3 \text{ s}^{-1}$  with temperature  $1100^\circ\text{C}$ .

increase in chamber overpressure and eruption rate. For the chamber located 10 km below the surface, we find that the basalt is actually unsaturated in volatiles for about 1 year, until there has been sufficient crystallization. Following this, the chamber pressure and eruption rate rapidly increase. Subsequently, as the silicic magma is heated up, it becomes volatile unsaturated, and the chamber pressure and eruption rate increase yet again.

[45] Figure 9c examines the sensitivity of the results to the fraction of the chamber volume occupied by the lower layer of basalt, which has been assumed to represent 10% of the chamber volume in the earlier calculations. Calculations are presented for the case in which there is no recharge, but in which both layers are volatile saturated, with total volatile budgets of 3 wt % (basalt) and 4 wt % (silicic) (compare Figure 7). As the fractional volume of basalt decreases, the rate of increase of pressure in the chamber also decreases, since there is a smaller total volume of gas being produced for a given cooling rate. Eventually, as the mass fraction of basalt decreases to very small values, the eruption behaves as if there is just a layer of compressible silicic magma which erupts from the chamber (Figure 4).

## 6. Conclusions and Discussion

[46] In this paper, we have developed a theoretical model to describe the evolution of an idealized two-layer magma chamber during a slow effusive eruption. The model accounts for the presence of exsolved volatiles in both the evolved layer of silicic magma, and also the new input of basaltic magma. We have found that the presence of exsolved volatiles, especially in the evolved and more massive layer of silicic magma, lowers the bulk modulus of the chamber by a factor of 10–100. The corresponding increase in compressibility can result in the eruption of 10–

100 times more material before the chamber overpressure has been relieved through eruption. If the potential eruption duration and total volume erupted is to be estimated from geophysical estimates of the volume of the magma chamber then our results suggest that it is key to estimate the degree of volatile saturation of the silicic magma in the chamber.

[47] The model allows for both (1) the possible recharge of the chamber with new basalt and (2) the cooling of the basalt and heating of silicic magma during the eruption. We have determined that for realistic values of case i the cooling rate of the basaltic magma, case ii the chamber volume, and case iii the eruption rate of silicic magma, then both the heat transfer between the basaltic and silicic magmas, and the eruption of silicic magma, may have an important effect on the evolution of the pressure in the chamber. In turn this has an important control on the ensuing eruption rate. If the basalt becomes saturated in volatiles, then as the basalt cools and crystallizes, it exsolves volatile gases. This tends to maintain the chamber pressure, leading to the possible eruption of a much larger volume of silicic magma. Indeed, during the initial stages of an eruption, in which the cooling rate may be the highest, the cooling of the basalt may lead to an increase in chamber pressure, thereby increasing the eruption rate (Figure 8). However, if the eruption is triggered and driven by the injection of a finite mass of basalt, then the eruption rate will gradually wane. In contrast, if there is a steady input of basalt during the eruption, then after the initial transient associated with the cooling, the system will tend to a state in which the eruption rate matches the sum of the input rate of magma and the rate of volume production resulting from heat transfer between the basaltic and silicic magmas.

[48] The model has not been designed to simulate specific events, or represent specific magmas, but to illustrate the wide range of possible evolution of the eruption rate during

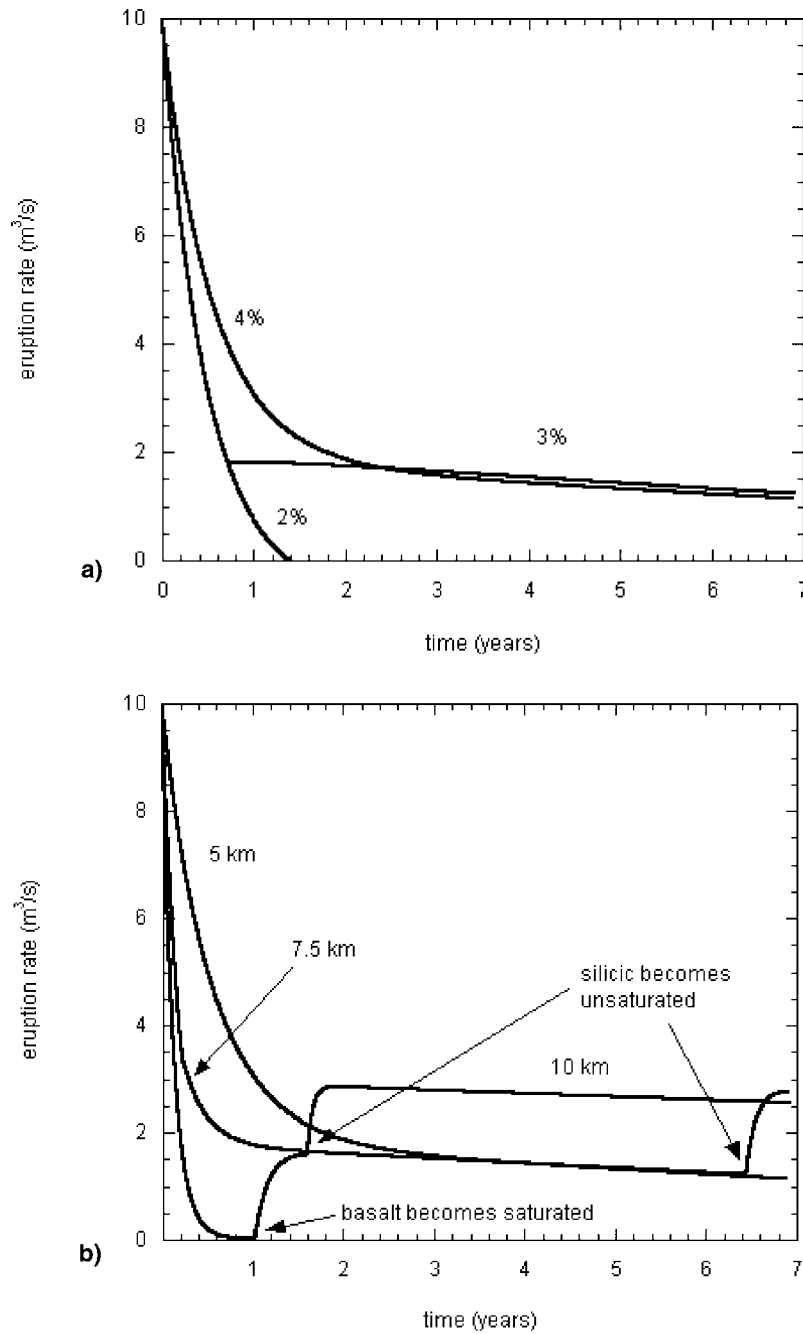


**Figure 9.** Variation of the model predictions as a function of (a) volatile content of the basalt (2, 3, and 4 wt %); (b) chamber depth (5, 7.5, and 10 km); and (c) fraction of the chamber occupied by the hot basaltic magma (0.01, 0.05, 0.1, and 0.2%).

a slow effusive eruption. The model predictions indicate this evolution is highly sensitive to the cooling rate, the size of the chamber, and the volatile contents of both layers of magma. However, as a general principle, the greater compressibility of a volatile rich magma, coupled with any cooling of the basalt, may lead to a nonmonotonic evolution of the eruption rate and an increase the erupted volume.

[49] There are many other controls on the eruption dynamics, some of which are associated with the variation of the magma density and rheology as it ascends the

conduit, owing to the decompression and exsolution of volatile gases [Jaupart and Allegre, 1991; Woods and Koyaguchi, 1994; Melnik and Sparks, 1999; Barmin et al., 2002]. For slow effusive flow, some of these complications in the conduit flow arise in the upper part of the conduit and dome, where the system may periodically become overpressured. This may lead to fluctuations in the surface eruption rate; indeed, field observations suggest variations over timescales ranging from days to years. In these more complex models of the conduit flow, the

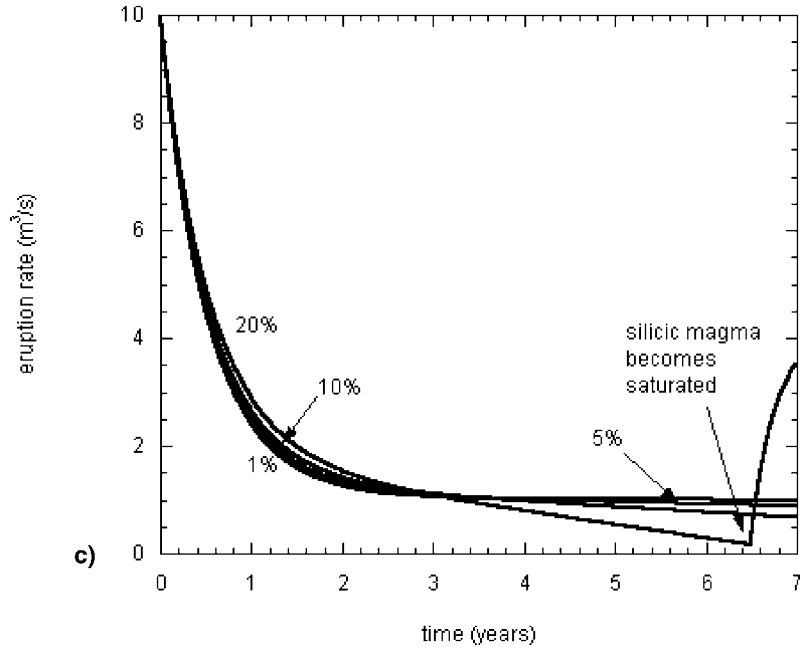


Figure 9. (continued)

transitions from one regime to another is largely controlled by the chamber pressure [Woods and Koyaguchi, 1994; Melnik and Sparks, 1999]. Therefore the evolution of the conditions in the source reservoir, as considered herein, is therefore likely to have a dominant control on the periodicity of transitions between different eruption regimes. In particular, the complex interplay of magma cooling and of the input/output of material can lead to nonmonotonic variations in chamber pressure. This is likely to lead to complex transitions in eruption regimes. We plan that this will be the subject of further study.

## Appendix A

[50] Here we use models of conductive and turbulent convective heat transfer to estimate some bounds on the rate of cooling of the basaltic magma. For high Rayleigh number turbulent convection [Turner, 1979] the heat transfer in a melt of depth  $h$  scales as

$$F_h \approx 0.1 \frac{\rho C_p \kappa \Delta T}{h} R_a^{1/3}. \quad (\text{A1})$$

Here the Rayleigh number,  $R_a = g_r \Delta \rho h^3 / \kappa \mu$ , where  $\kappa$  is the thermal diffusivity. For small Rayleigh numbers, smaller than about  $10^6$ , the magnitude of the heat flux gradually reduces to the purely conductive scaling  $F_h \approx \rho C_p \kappa \Delta T / h$ . If the basalt-silicic magma system is convecting, with a heat flux from the hot basalt (1300°C) to the cooler silicic magma (750–850°C), then the two fluxes are equal. Since the viscosity ratio of the two magmas may be of order  $10^3$ – $10^6$ , then, if the depth ratio is of the order of 10–100, the convection in the silicic magma tends to limit the heat transfer between the two bodies of magma. As a result, the temperature difference between the two bodies of magma will be largely accommodated in the boundary layer in the silicic magma. For a 100–1000 m layer of silicic magma of viscosity  $10^7$  Pa s, this would imply a  $R_a$  number of order

$10^8$ – $10^{11}$ , and a heating rate about  $10^{-5}$ – $10^{-8}$  °C s<sup>-1</sup>. The associated cooling rate of the basalt would then be in the range  $10^{-7}$ – $10^{-4}$  °C s<sup>-1</sup> for a 10 m deep layer. In the main text, we use a cooling rate of order  $10^{-6}$  °C s<sup>-1</sup> for the basalt and examine how the model predictions change as the cooling rate varies from this value.

[51] **Acknowledgments.** We are extremely grateful to Steve Sparks, who has given many invaluable suggestions about this topic and has carried out thorough reviews of several drafts of the paper. We also thank Ross Kerr, an anonymous referee, and Larry Mastin for their reviews of this work.

## References

- Barmin, A., O. Melnik, and R. S. J. Sparks, Periodic behaviour in lava dome eruptions, *Earth Planet. Sci. Lett.*, **199**, 173–184, 2002.
- Blake, S., Volcanism and the dynamics of open magma chambers, *Nature*, **289**, 783–785, 1981.
- Blake, S., Volatile oversaturation during the evolution of silicic magma chambers as an eruption trigger, *J. Geophys. Res.*, **89**, 8237–8244, 1984.
- Bower, S., and A. W. Woods, Control of magma volatile content and chamber depth on the mass erupted during explosive volcanic eruptions, *J. Geophys. Res.*, **102**, 10,273–10,290, 1997.
- Cardoso, S. S. S., and A. W. Woods, On convection in a volatile-saturated magma, *Earth Planet. Sci. Lett.*, **168**, 301–310, 1999.
- Druitt, T., and R. S. J. Sparks, On the formation of calderas, *Nature*, **310**, 679–681, 1984.
- Eichelberger, J., C. R. Carrigan, H. R. Westrich, and R. H. Price, Non-explosive silicic volcanism, *Nature*, **323**, 598–602, 1986.
- Folch, A., and J. Marti, The generation of overpressure in felsic magma chambers by replenishment, *Earth Planet. Sci. Lett.*, **163**, 301–314, 1998.
- Holloway, G., and M. Carroll (Eds.), *Volatiles in Magmas*, *Rev. Mineral.*, Mineral. Soc. of Am., Washington, D. C., 1994.
- Huppert, H. E., and R. S. J. Sparks, The generation of granitic magmas by intrusion of basalt into continental crust, *J. Petrol.*, **40**, 241–254, 1988.
- Huppert, H. E., J. S. Turner, and R. S. J. Sparks, Effects of volatiles on mixing in calc-alkaline magma systems, *Nature*, **297**, 554–557, 1982.
- Jaupart, C., Gas loss from magmas through conduit walls during eruption, in *The Physics of Explosive Volcanic Eruptions*, edited by J. S. Gilbert and R. S. J. Sparks, *Geol. Soc. Spec. Publ.*, **145**, 73–90, 1998.
- Jaupart, C., and C. Allegre, Gas content, eruption rate and instabilities of eruption in silicic volcanoes, *Earth Planet. Sci. Lett.*, **102**, 413–429, 1991.

- Melnik, O., and R. S. J. Sparks, Nonlinear dynamics of lava dome extrusion, *Nature*, 402, 37–41, 1999.
- Sparks, R. S. J., The dynamics of bubble formation and the growth in magmas—A review and analysis, *J. Geophys. Res.*, 83, 1–37, 1978.
- Sparks, R. S. J., H. Sigurdsson, and L. Wilson, Magma mixing: A mechanism for triggering acid explosive eruptions, *Nature*, 267, 315–318, 1977.
- Sparks, R. S. J., et al., Magma production and growth of the lava dome of the Soufriere Hills volcano, Montserrat, West Indies, November 1995 to December 1997, *Geophys. Res. Lett.*, 25, 3421–3424, 1998.
- Stasuik, M., R. S. J. Sparks, and C. Jaupart, On the variations of flow rate in non-explosive lava eruptions, *Earth Planet. Sci. Lett.*, 114, 505–516, 1993.
- Tait, S., C. Jaupart, and S. Vergnolle, Pressure, gas content and eruption periodicity of a shallow, crystallising magma chamber, *Earth Planet. Sci. Lett.*, 92, 107–123, 1989.
- Timoshenko, S. P., and J. N. Goodier, *Theory of Elasticity*, 3rd ed., 567 pp., McGraw-Hill, New York, 1970.
- Touloukian, Y. S., W. R. Judd, and R. F. Roy (Eds.), *Physical Properties of Rocks and Minerals*, vol. 1, 548 pp., McGraw-Hill, New York, 1981.
- Turner, J. S., *Buoyancy Effects in Fluids*, Cambridge Univ. Press, New York, 1979.
- Wadge, G., The variation of magma discharge during basaltic eruptions, *J. Volcanol. Geotherm. Res.*, 11, 139–168, 1978.
- Woods, A. W., and T. Koyaguchi, Transitions between explosive and effusive eruptions of silicic magma, *Nature*, 370, 641–644, 1994.
- Woods, A. W., and D. Pyle, The control of chamber depth on eruptions triggered by cooling and crystallisation of magma, *Earth Planet. Sci. Lett.*, 151, 155–166, 1997.

---

H. E. Huppert and A. W. Woods, BP Institute and Institute for Theoretical Geophysics, Madingley Rise, Madingley Road, Cambridge CB3 0EZ, UK. (andy@bpi.cam.ac.uk)